TECHNICAL FINAL REPORT

Imaging Fault Structures Near the Imperial Fault in the All American Canal

1 PROJECT OVERVIEW

1.1 ABSTRACT

We employed an acoustic high-resolution, shallow imaging technique (CHIRP) in the All American Canal (AAC) by the US-Mexico border to provide direct constraints on near-surface splays of the Imperial Fault (IF), and other structures to its west. The Imperial Fault is a high slip-rate fault within the context of Southern California tectonics, yet there are few paleoseismic studies due to agricultural obfuscation of surface faulting. Our goal was to directly image near-surface structures on and near the IF to understand better local fault interactions, and direct future paleoseismic studies for improved slip rates. Current results have shown some shallow deformation near the area of the mapped IF surface trace, as well as offset strata and significant distributed deformation in an area approximately 10 to 23km west of the mapped IF trace. We interpret that this corresponds to deformation associated with the northern extension of the Michoacán fault, as well as structures associated with a stepover between the Michoacán and Dixieland Faults.

SCEC Annual Science Highlights FARM, CFM

SCEC Science Priorities P1.a, P3.a, P5.b, P5.c

1.2 INTELLECTUAL MERIT

Our findings are:

- We image deformation of strata due to the Imperial Fault, both in the shallow surface and below ~ 15m depth.
- We resolve significant deformation (~4.5m) near the northward extension of the Michoacán fault, corresponding with lineaments of seismicity and structures proposed by Magistrale [2002] and Lindsey and Fialko [2016].
- We see offset strata, and significant and distributed deformation in an area approximately 10 - 23km west of the Imperial Fault, between the Michoacán and Dixieland faults, likely due to shallow deformation within the transtensional stepover.

1.3 BROADER IMPACTS

The results from this work suggest that surface faulting or shallow deformation may be more distributed in this region than is represented in hazard models. Shallow constraints like those provided by our data will be helpful in a number of ways. They will allow future workers to

target ideal locations for further studies such as trenching, to obtain direct geologic slip rate estimates on these fault zones. They will also help in defining fault structures in the region besides the IF to include in modeling studies. Additionally, this work will contribute to our understanding of the interactions between faults in this region and how they may impact estimates of seismic hazard.

2 Technical Report

2.1 Introduction

Obtaining a complete image of active faulting in Southern California is important for understanding present-day fault interactions and seismic hazard, as well as for elucidating how this complex and segmented margin has evolved through time. At the latitude of the US-Mexico border, the Imperial Fault (IF) has often been considered as the major player in the Pacific-North American plate boundary system. Two large earthquakes (1940 **M**7.0 and 1979 **M**6.5) have occurred on this fault in the past century, and geodetic and hazard models such as the Uniform California Earthquake Rupture Forecast version 3 (UCERF3, Field et al. [2014]) attribute 30-40mm/yr of plate boundary slip to this fault. This is contested, however, by paleoseismic, seismicity, and more recent geodetic studies, which suggest there are likely several other active faults in the region.

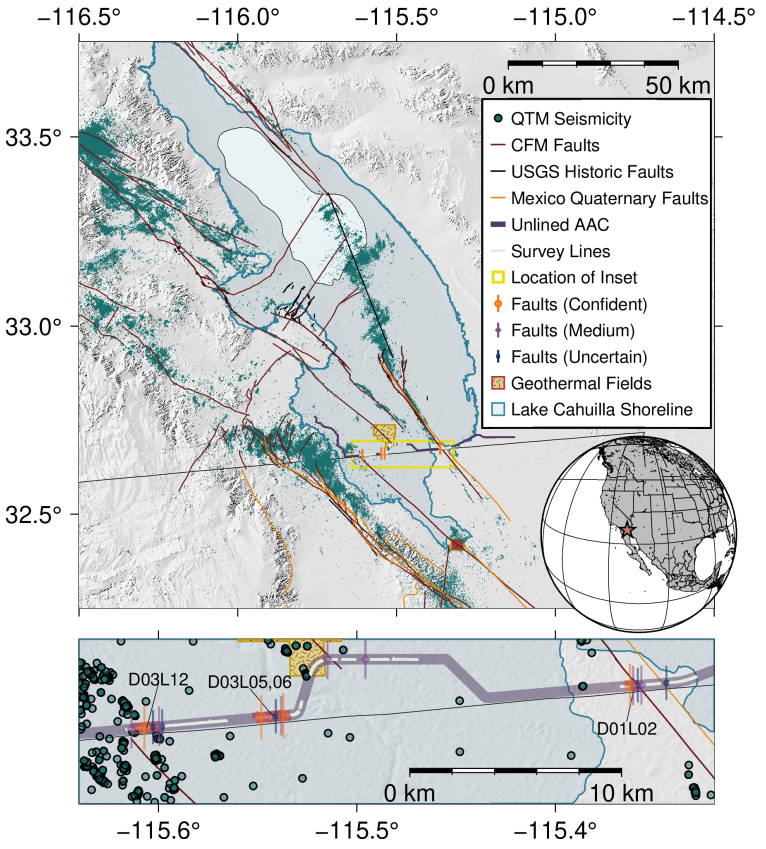

Figure 1: Regional map showing the Salton Trough and Imperial Valley. Inset is of the All American canal and location of study. Fault and deformation interpretations are shown, as well as the selected lines shown as figures in this study. Seismicity is from the Quake Template Matching Catalog of Ross et al. [2019], faults are the SCEC community fault model (CFM) faults.

Geologic slip rates on the IF are much lower, 15 – 20mm/yr near the border [Thomas and Rockwell, 1996]. Patterns of seismicity in the Imperial Valley propose that a number of other faults share the plate boundary strain with the IF, including the Weinert-El Centro and Dixieland faults, as well as the Michoacán/Tule Check fault which is the northern extension of the Cerro Prieto fault [Magistrale, 2002, González-Escobar et al., 2020]. North of the US-Mexico border, recent geodetic studies such as Lindsey and Fialko [2016] have used InSAR and GNSS data to place less slip on the IF in the Imperial Valley, and more on a structure 10-20km to its

west. The IF slip rate decreases towards the border, with a second fault accommodating more of its motion. South of the border, recent geodetic work shows that several faults across the region accommodate plate motion, including the IF, Sierra Cucapah, and Tule Check/Michoacán faults (Sandwell et al., 2016).

Others have previously suggested that the Michoacán fault likely extends north of the border, taking some of the region's slip, or that southern extension of the Superstition Hills fault may accommodate some of the remaining slip [Thomas and Rockwell, 1996, Magistrale, 2002]. Furthermore, new mechanical models in the region [Dorsett et al., 2019] found that the Cerro Prieto/Michoacán fault is likely linked to the Imperial Fault system, and that faults such as the Dixieland fault accommodate some of the IF's slip rate, bringing the IF slip rate closer to geologic estimates. However, there are no paleoseismic sites on the Michoacán fault in the US, and few others in the region. The El Centro/Mexicali area near the border and these faults is particularly challenging for tectonic studies. Geomorphic evidence of faulting is almost entirely obscured due to anthropogenic activity, and identifying suitable sites for paleoseismic trenches is also difficult. Several exist, including Jerrett [2016] and Sharp (1980) north of the border, Thomas and Rockwell [1996] south of the border, but overall the geologic slip rate is not as well constrained as other faults in the Southern California region.

A more detailed understanding of the location of fault structures – in both the shallow surface and at depth – are important for understanding better the interactions between fault structures in this region. Important to know if faults can/likely to link up, as well as understand the evolution of the margin. To constrain deformation in the shallow subsurface, we conducted a novel study, using a traditionally marine subsurface imaging instrument in the All American Canal (AAC) in the Imperial Valley. The AAC is a large aqueduct, transporting water from the Colorado River northeast of Yuma, AZ to the Imperial Valley, California. Along its traverse, the AAC runs parallel to the California/Mexico border by Calexico, CA, and directly cross the Imperial Fault, Dixieland fault, and proposed region of strain accommodation (Figure 1). By using a marine high-resolution subbottom imaging system in the unlined section of the AAC, crossing the IF, we image shallow deformation which we attribute to these structures, and use to constrain slip rates, interaction of fault structures in the region.

Figure 2: Images showing deployment of the CHIRP. Left: Bottom of the CHIRP, with transducers. Top right: The CHIRP in its cage, with one floating pontoon mounted. Bottom right: The CHIRP during the deployment process, with Septentrio receiver mounted on the frame.

2.2 Data & Methods

Campaign planning Completion of permitting processes occurred in Fall 2018 - Winter 2019. The permits required for this study included an encroachment permit from the Imperial Irrigation District (IID), and a temporary use permit from the Bureau of Reclamation (BOR). Survey planning occurred in Winter 2019, including coordination with the IID and BOR's maintenance schedule, as well as clearance from the Department of Homeland Security (DHS), and U.S. Customs and Border Protection, as the All American Canal parallels the border closely. Survey lines were planned to cross the mapped section of the IF, as well as lines between approximately 10 and 20km to the west of the IF which coincide with the region of a proposed fault from Lindsey and Fialko [2016], as well as observed seismicity lineaments.

Data Collection

We collected the majority of the planned survey lines, as time constraints allowed. To image shallow deformation structures, we used an acoustic compressed high intensity radar pulse (CHIRP) instrument, by exploiting the aqueous environment of the canal as a substrate for imaging. Acoustic compressed high intensity radar pulse (CHIRP) data provides high-resolution images of subsurface stratigraphy in marine environments, by sending modulated frequency pulses of acoustic energy through water, and receiving reflected energy on a collocated receiver. Using two trucks on the banks of the AAC (Figure 2), we towed an Edgetech SubScan JSTAR CHIRP with a dual-transducer XStar sonar through approximately the center of the canal. With the CHIRP in a floating cage, we placed a Septentrio Altus NR3 GNSS instrument on top of the CHIRP with a 1Hz sample rate to obtain real-time, sub-meter positioning information on the seismic data. For maximum penetration, we used a 50ms 0.7 – 3.0 kHz swept frequency pulse with 3 pulses per second, to increase coherency from reflections from subsurface structures. Previous pilot studies we conducted in this region demonstrated that higher frequencies do not adequately resolve stratigraphy beyond ~ 10 meters below the surface, due to highly reflective canal bedforms. This lower frequency pulse allowed us to image, with decent resolution, down to 20 - 30m beneath the canal bed. See Figure **??** for line locations.

Intermittent grates in the canal prevented us from towing the CHIRP in the traditional way with a vessel, and required a novel approach. The IID provided us with the use of their crane truck and operator time to deploy and recover the CHIRP in the canal, and assisted us with the deployment. In order to tow the CHIRP in the canal without a vessel, we placed the instrument in a floating cage, and once deployed in the canal, pulled it against the canal current using a truck on both canal banks (figure 2).

Typically, navigation is performed using a Garmin 17HVS mounted on the towing vessel, and the CHIRP's position is determined based on the towing distance behind the vessel. Our unique survey configuration required us to mount a Septentrio Altus NR3 positioning antenna and receiver on a pole on the CHIRP's floating frame, while simultaneously running the Garmin 17HVS to track the position of the tow truck. Positioning written to the raw files was from the Garmin instrument, and positions from the NR3 were later substituted per shot into the segy files.

We collected these data in three main regions: (1) near the IF mapped trace at the CA/Mexico border, (2) in the center of Calexico near a jog in the AAC, intersecting with the mapped trace of the Dixieland Fault and approximately located 5km west of the mapped trace of the Weinert fault; and (3) approximately 23km west of the mapped IF trace, near the Cerro Prieto fault. In total, we collected 27 lines.

Data Processing

Standard CHIRP processing was applied to this data. Data are produced in .jsf format, a proprietary EdgeTech convention. Onboard the instrument, signals are match filtered to com-

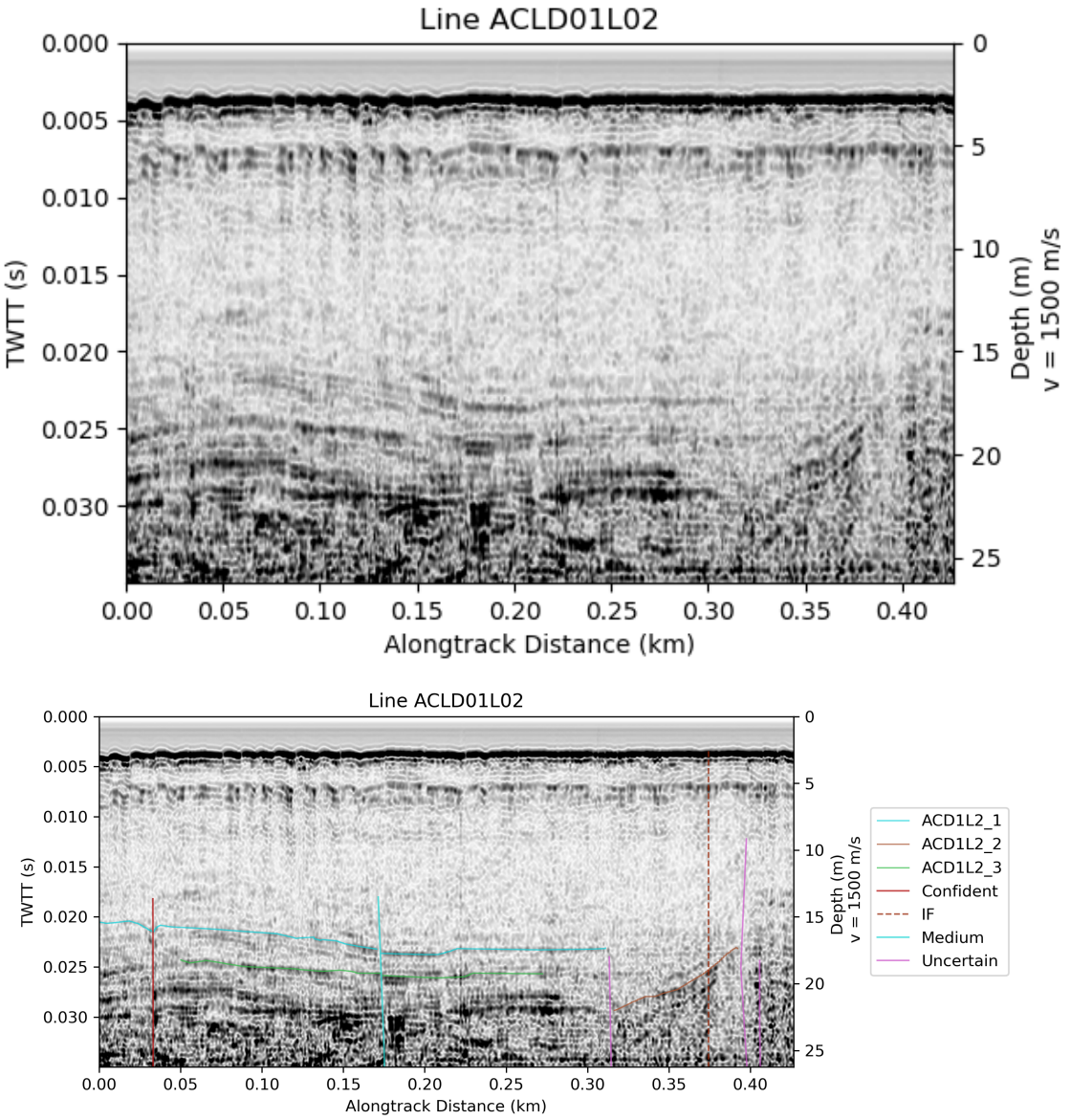

Figure 3: Line ACLD01L02 from survey section 1. Top: uninterpreted, showing deformation of thick, continuous reflectors, at approximately 0.30 to 0.40km alongtrack distance, 15 - 25m depth and gently dipping reflectors at the same alongtrack distance and approximately 1m beneath the canal bed. Dashed line shows the UCERF3 mapped trace of the IF

press and remove the source signature, significantly improving the resolution of the data and clarity of subsurface reflectors. We converted these match filtered .jsf files to .segy files, and applied a heave correction (though mostly unnecessary on these data as the canal conditions were calm). Then, to associate the accurate Septentrio Altus NR3 navigation data with each lines' shots, we matched the timestamps of each pulse with timestamps from the NR3 NMEA file, and replaced the individual trace headers with their accurate shot location. Finally, we applied a time-varying gain and automatic gain control to increase the coherency and clarity of deeper reflectors.

Data Resolution and Clarity

In the first region, the eastern lines that cross the IF, the CHIRP pulse depth penetration seemed to be lower, and resulted in lower amplitude reflectors at depths >10 - 15m. We applied a greater gain to these lines to increase the clarity of these reflectors. The easternmost lines in the first region showed striping and obfuscation of reflectors from gas, from the canal bed to the depth limit of the data. The second and third survey sections, the depth penetration of the CHIRP improved, necessitating a lower gain for these lines. There was still gas observable on these lines - in some cases it appears as striping on the lines, obfuscating reflectors from the canal bed to the depth limit of the data, and in other cases the obfuscation is limited to the deeper section of the data, and shallow reflectors are still clear. Some of the lines in the third section show the greatest coherency in reflectors, with the most interpretable data.

2.3 Results

We qualitatively characterize our faulting and deformation interpretations by "confident" (obvious offset) "medium confidence" (offsets with moderate clarity, and/or deformation likely controlled by a fault structure) and "uncertain" (deformation or offsets with low to moderate clarity). Overall, observing surface deformation of the canal bed is challenging in many places. The top 0 - 5 meters, depending on the line, is obscured by bedforms produced by the canal current. In survey section 1, we find obvious deep deformation of strata near the mapped trace of the IF (line ACD01L02). These lines exhibit thick, continuous reflectors that are folded at 15 - 25m depth (Figure 3). In addition on this line, we see slight deformation of the near-surface layers, near approximately 2m beneath the canal floor. These dip away from the mapped IF trace, to the apparent southwest and northeast. Near the mapped trace at intermediate depths there is striping from gas, but deep strata dip away from both sides of the striping. In other lines in survey section 1, these same thick and continuous reflectors are mostly flat-lying.

In survey region 2, we observe some shallow deformation and folding of reflectors above 10m depth, however here the reflectors are thinner and less continuous in comparison to survey region 1. Identifying surface offsets here is challenging because though there are no bedforms, the reflectivity of the canal floor is high. Gas is prevalent in this region, and the time-varying gain enhances canal floor multiples at depths greater than approximately 15m. Here, the com-

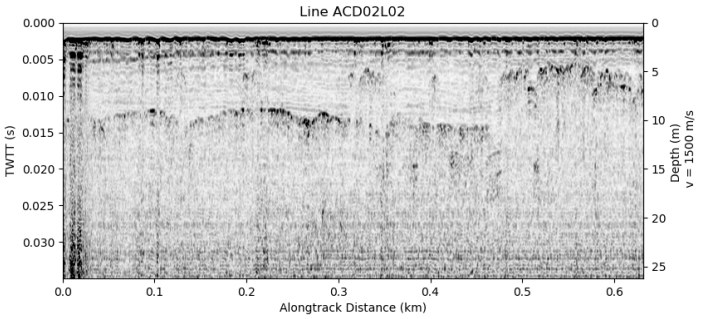

Figure 4: Line ACD02L02 from survey section 2 showing shallow deformation of reflectors, above 10m depth.

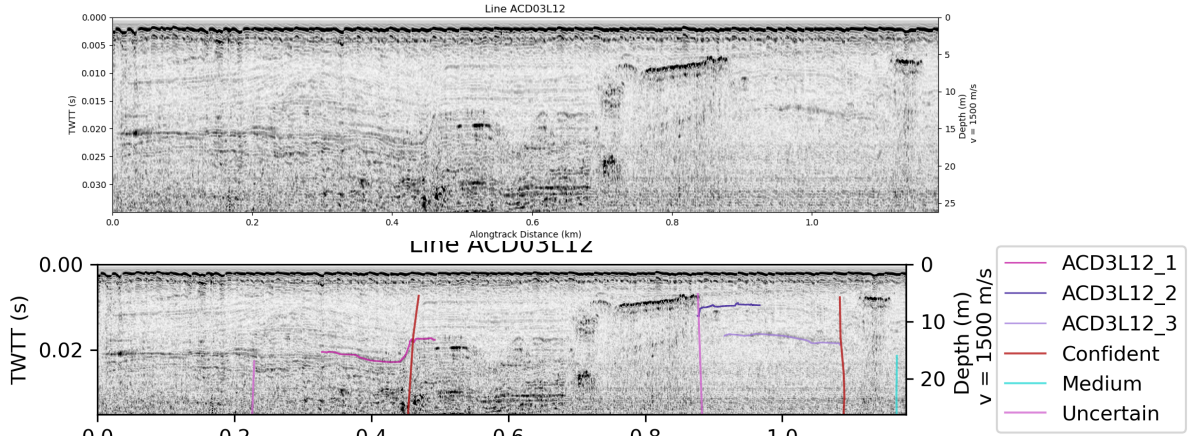

Figure 5: Line ACD03L12 from survey section 3. Top: Uninterpreted profile showing pronounced deformation of reflectors, from 25m to nearly the surface. Bottom: Interpreted profile.

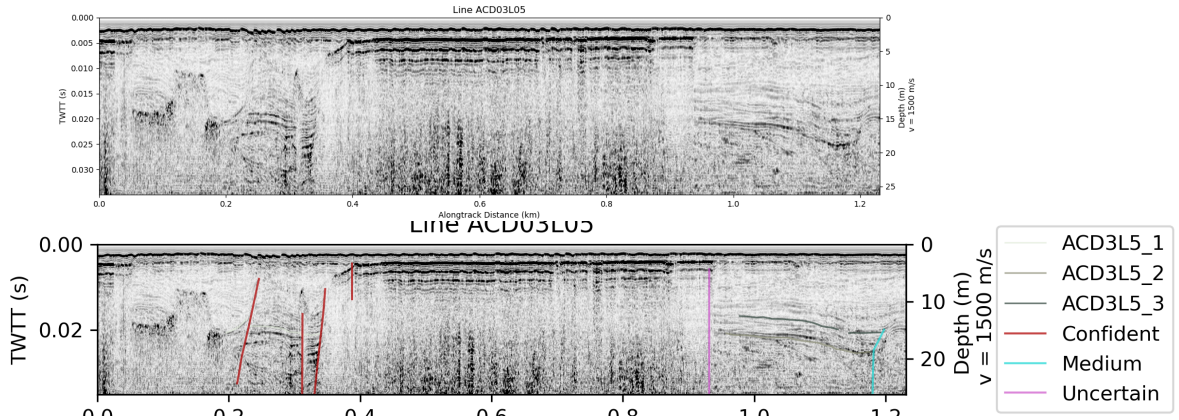

Figure 6: Line ACD03L05 from survey section 3. Top: Uninterpreted profile showing pronounced deformation of reflectors, from 25m to nearly the surface. Bottom: Interpreted profile.

bination of these two artifacts obscures deformation below ~10m on many lines. Most observable reflectors in this region are flat-lying.

The mapped trace of the Dixieland Fault coincides with line ACD02L01(Figure 1), though cannot make any interpretations here due to the strong prevalence of gas. Approximately 200m to the west, we see some small deformation and offsets in reflector ACD2L1_1, with an overall westward dip of 2.75 degrees. Approximately 1km to the west on line ACD02L03, we have a structure mapped with medium confidence, and near surface offsets. This coincides with a canal bedform, however demonstrates offset of reflectors down to ~5m depth, greater than the other bedforms in the region.

The most pronounced observations of faulting occur in survey region 3. Clear offsets in reflectors are observed here, in addition to continuous, deformed reflectors. We observe these features on lines ACD03L05, ACD03L06, ACD03L12, and ACD03L13. In the westernmost portion of Region 3 (near the seismicity lineament of the Michoacán Fault), line ACD3L11 demonstrates splay faulting with offsets in reflectors, approximately 1.3m in reflector ACD3L11_2. We

observe clear offsets in reflectors on line ACD03L12 with down-to-the-west motion (Figure 5). The total vertical offset across this interpreted fault is nearly 4m. Further east along this line, there is an abrupt transition between continuous reflectors and chaotic reflectors, interpreted as a "confident" fault. There is a prominent region of gas in the middle of this line, which separates mostly flat-lying reflectors, and dipping reflectors, leading to the interpretation of an "uncertain" fault.

Other lines in this region are not interpretable due to gas, however the gas on line ACD03L13 occurs primarily in the middle of the line, with reflectors dipping and thickening towards the center region of gas, leading to the interpretation of two "uncertain" faults surrounding this region, though the structure causing this deformation may be obscured by gas.

Finally, lines ACD03L05 and 06 show clear faulting. The "confident" fault interpreted on the western-most section of line ACD03L05 demonstrates offset >1m of reflectors, and the adjacent fault warps reflectors, though continuity of these is not sufficient enough to confidently describe an offset. The easternmost section of this line shows folded reflectors, and is immediately adjacent to line ACD03L06, which shows divergence of reflectors, small offsets, and a westward dip in between two confidently mapped faults. Reflector ACD3L1_1 falls in towards the westernmost fault on this line with a dip of 8 degrees.

2.4 Discussion

The deformation in survey section 1 coincides with the mapped surface trace of the IF, and likely represents deformation from the IF from both the 1940 and 1979 events, as well as possibly previous events. Both the deeper strata surrounding the mapped fault trace, and the shallower strata exhibit the same southwestward tilt as beds noted in the trenches of Sharp (1980) [Thomas and Rockwell, 1996] very nearby our site (<1km), suggesting that these structures are not just very local, but rather a more pervasive feature within the few hundred meters surrounding the border. Just near our interpreted, and the previously mapped, IF, reflectors are obscured by significant gas. A lack of surface deformation in this area could indicate that offsets from the fault do not reach the surface, but they could also be obfuscated by gas.

Section 3 shows the most compelling evidence of shallow deformation, and in particular provides the first ever images of shallow faulting in this region to the west of the IF. We see two distinct areas of section 3 with faulting. The first is in the western lines of survey section 3 are within the postulated location of the northern extension of the Michoacán fault. The offsets on reflectors in this region are comparable if not larger than those observed across the IF in survey section 1; in fact the vertical offsets on the westernmost structure of ACD03L12 (Figure 5) shows approximately 4.5 meters of vertical offset. The second area of faulting in section 3 is observed on lines ACD03L05 and 6, to the east of ACD03L11 and 12. We see transtensional faulting features here, both at greater depths and the shallow surface. We cannot resolve surface faulting of these strata.

Observing shallow faulting in this region is not unexpected. Previous workers in the area proposed that the Michoacán fault likely extends to the north, based on partitioning of slip rates and observed seismicity lineaments. They also suggested that the Dixieland fault accommodates some plate boundary strain here [Magistrale, 2002, Lin et al., 2007, Jennings et al., 2010, Lin, 2013, Nicholson et al., 2017]. Recent mechanical modeling work from Dorsett et al. [2019] finds that the Michoacán fault and Cerro Prieto fault are likely linked to the Imperial Fault system, and that faults such as the adjacent Dixieland fault accomodate approximately 3 and 8 mm/yr of slip rate. This would re-partition some of the UCERF3 IF slip rate onto the Dixieland fault, and partly the Michoacán fault. Furthermore, Lindsey and Fialko [2016] places between 10 and 15 mm/yr of slip on a structure or structures at this approximate longitude.

We propose that the deformation in the western area of section 3 on lines ACD03L11 and 12 are the surface manifestation of slip associated with the northern extension of the Michoacán fault, observable in seismicity. While unsurprising, this structure is yet to be investigated north of the US-Mexico border, and is not included in current fault models. We additionally propose that the transtensional structures we observe in the eastern area of section 3, on lines ACD03L05 and 6, are associated with the Michoacán to Dixieland fault stepover. There is no seismicity here (Figure 1), so we propose that these structures are likely created during rupture on either the Michoacán or Dixieland fault, or potentially during throughgoing ruptures between the two faults and through the stepover. With a two-dimensional dataset limited by the location of the canal, it is not possible for us to propose any further constraints on the possibility of throughgoing rupture. Additionally, along survey section 2, small amounts of deformation are difficult to attribute to the Dixieland fault due to gas.

Lastly, this dataset cannot provide direct slip rates on any observed structures. We lack cores in the area to date sediments, and it is challenging to say with any certainty that particular reflectors are associated with previous lake highstands (which would place additional age constraints on the observed deformation). We are, however, working with Professor Tom Rockwell at SDSU to corroborate our active-source images and amplitudes with similar depth data collected via drilled cores, and CPT lines. This may allow us to place wide constraints on the age of the observed faulting near the mapped IF trace.

2.5 Conclusions

Our dataset provides some of the first images of subsurface deformation on the Imperial fault at the US-Mexico border, and the first images of subsurface deformation on structures to its west. It confirms that the Michoacán or Cerro Prieto fault extends northwards into the US, and aligns with lineaments of observed seismicity. We see transtensional structures in the region between the Michoacán and Dixieland faults, indicative of possible coseismic displacements in the stepover between these faults. We can neither confirm nor deny the possibility that these occurred during throughgoing rupture in previous events, but it is possible based on mechanical modeling in the region [Dorsett et al., 2019] that suggests interaction between these two structures. We cannot place slip rates on these structures as we do not have direct samples of the imaged strata, however this work will provide valuable constraints on the locations of future studies, to better understand regional slip rates and fault interactions in the Imperial Valley.

2.6 Project Presentations

1. Sahakian, V. J., Driscoll, N. W., Derosier, B., Rockwell, T., Stock, J. M., & Driscoll, N.W. (2021). *Shallow Deformation Features of the Imperial and Michoacán Fault Systems From Subsurface Imaging*, Oral Presentation at 2021 SSA Annual Meeting.

2. Sahakian, V. J., Derosier, B., Stock, J. M., & Driscoll, N.W. (2020). *Shallow Deformation Features of the Imperial Fault System from Subsurface Imaging*, Oral Presentation at 2020 Reunión Anual UGM.

3. Sahakian, V. J., Driscoll, N. W., Derosier, B., Oller, B., Klimasewski, A. R., & Stock, J. M. (2019). *Shallow Surface Deformation on the Southern Imperial Fault System from Marine Subsurface Imaging Data*, Poster Presentation at 2019 SCEC Annual Meeting.

3 Planned Dissemination and Future Use of Results

Submission of a publication of the results is in preparation for *Geology*, with planned submission in March 2021. We are completing a corroboration study between our active-source data, and nearby cores and CPT data collected by Tom Rockwell. To disseminate the raw and processed data, CHIRP data will be submitted to the UTIG seismic data portal concurrent with publication. Data resulting from interpretation in this study such as maps of deformation and interpreted fault structures will be placed in Kingdom Suite files, Google Earth .kmz files, as well as ASCII files, and will be submitted to Zenodo with a DOI that will accompany publication.

The results of this study will be helpful in identifying future trenching and other geologic study sites in the region, as well as constraining future modeling studies. This will help constrain the slip rates on the observed faulting structures, as well as help to understand the interactions between fault structures such as the IF, Dixieland fault, and Michoacán fault.

References

Jacob H Dorsett, Elizabeth H Madden, Scott T Marshall, and Michele L Cooke. Mechanical models suggest fault linkage through the imperial valley, california, usa. *Bulletin of the Seismological Society of America*, 109(4):1217–1234, 2019.

Edward H Field, Ramon J Arrowsmith, Glenn P Biasi, Peter Bird, Timothy E Dawson, Karen R Felzer, David D Jackson, Kaj M Johnson, Thomas H Jordan, Christopher Madden, et al. Uniform california earthquake rupture forecast, version 3 (ucerf3)—the time-independent model. *Bulletin of the Seismological Society of America*, 104(3):1122–1180, 2014.

Mario González-Escobar, Miguel Angel Mares Agüero, and Arturo Martin. Subsurface structure revealed by seismic reflection images to the southwest of the cerro prieto pull-apart basin, baja california. *Geothermics*, 85:101779, 2020.

Charles W Jennings, William A Bryant, and G Saucedo. Fault activity map of california. *California Geological Survey Geologic Data Map*, 6, 2010.

Andrew Steven Jerrett. *Paleoseismology of the Imperial Fault at the US-Mexico Border, and correlation of regional lake stratigraphy through analysis of oxygen/carbon isotope data*. PhD thesis, Sciences, 2016.

Guoqing Lin. Three-dimensional seismic velocity structure and precise earthquake relocations in the salton trough, southern california. *Bulletin of the Seismological Society of America*, 103 (5):2694–2708, 2013.

Guoqing Lin, Peter M Shearer, and Egill Hauksson. Applying a three-dimensional velocity model, waveform cross correlation, and cluster analysis to locate southern california seismicity from 1981 to 2005. *Journal of Geophysical Research: Solid Earth*, 112(B12), 2007.

Eric O Lindsey and Yuri Fialko. Geodetic constraints on frictional properties and earthquake hazard in the imperial valley, southern california. *Journal of Geophysical Research: Solid Earth*, 121:1097–1113, 2016. doi: 10.1002/2015JB012516.

Harold Magistrale. The relation of the southern san jacinto fault zone to the imperial and cerro prieto faults. *SPECIAL PAPERS-GEOLOGICAL SOCIETY OF AMERICA*, pages 271–278, 2002.

C Nicholson, A Plesch, and JH Shaw. Community fault model version 5.2: Updating & expanding the cfm 3d fault set and its associated fault database. In *Poster Presentation at 2017 Southern California Earthquake Center (SCEC) Annual Meeting*, 2017.

Zachary E Ross, Daniel T Trugman, Egill Hauksson, and Peter M Shearer. Searching for hidden earthquakes in southern california. *Science*, 364(6442):767–771, 2019.

Andrew P Thomas and Thomas K Rockwell. A 300-to 550-year history of slip on the imperial fault near the us-mexico border: Missing slip at the imperial fault bottleneck. *Journal of Geophysical Research: Solid Earth*, 101(B3):5987–5997, 1996.